Received March 24, 2021, accepted April 2, 2021, date of publication April 7, 2021, date of current version April 19, 2021.
Digital Object Identifier 10.1109/ACCESS.2021.3071616

Sensor Fault Diagnosis and Fault Tolerant Control for Automated Guided Forklift

HANGUO KANG, BENXIAN XIAO, YOYUAN NI, WEIDONG JIANG, (Member, IEEE), JINPING WANG, (Member, IEEE), ZHENG SUN, AND ZHILU ZHANG
School of Electrical Engineering and Automation, Hefei University of Technology, Hefei 230009, China
Anhui Province Engineering Technology Research Center of Industrial Automation, Hefei University of Technology, Hefei 230009, China
Corresponding author: Benxian Xiao (xiaobenxian@126.com)

This work was supported in part by the National Natural Science Foundation of China under Grant 51577046, and in part by the Hefei Banyitong Science and Technology Development Company Ltd.

ABSTRACT For the problem of multiple sensor faults in the automated guided forklift (AGF), an equivalent model with system faults and disturbances is established. To detect multiple sensor faults in the AGF, a sliding mode observer (SMO) is proposed. It introduces a fault estimation algorithm that is designed by the fault residual and the residual is only sensitive to sensor faults which means that the SMO is robust to unknown input disturbances. On the other side, it can also judge the faulty sensor according to the feature vector of different sensors. To judge the type of sensor faults accurately, a mathematical model of sensor fault characteristics is established and it can provide a foundation for choosing appropriate fault-tolerant output compensation measures. Then an active fault-tolerant control method based on state feedback is proposed. It can restore the control system to normal and maintain the stability of the control system. Finally, experiments are given to verify the effectiveness of the proposed fault-tolerant control strategy.

INDEX TERMS AGF, sensor fault, fault diagnosis, fault tolerant control, SMO.

I. INTRODUCTION

The wide application of AGF is conducive to the establishment of an intelligent logistics system and improving logistics efficiency. Correspondingly, greater demands are being placed on the reliability of the control system, especially the fault detection of primary sensors and fault-tolerant of the system.

The fault diagnosis and tolerant control techniques of vehicles have been intensively investigated. In [1], a fault diagnosis approach for finding the faulty in-wheel motor/motor driver pair is developed, and based on the in-wheel motor/motor driver faults diagnosis mechanism, a control-allocation based vehicle fault-tolerant control system is designed to accommodate the in-wheel motor/motor driver faults by automatically allocating the control effort among other healthy wheels. For the path-tracking problem for four-wheel-steering and four-wheel-driving electric vehicles with input constraints, actuator faults, and external resistance, a hybrid fault-tolerant control approach, which combines the linear-quadratic control method and the control Lyapunov function technique, is proposed [2]. However, few contributions have been made for the fault diagnosis and tolerant control of AGF.

For the model uncertainties, a SMO, which introduces a fault estimation algorithm with adaptive law, is proposed. The SMO has been widely applied to cope with this problem. An adaptive-gain second-order sliding mode (SOSM) observer is developed for observing the PEM (polymer electrolyte membrane) fuel cell system states, where the adaptive law estimates the uncertain parameters [3]. In [4], a new delay-derivative-dependent SMO design for a class of linear uncertain time-varying delay systems is presented. Moreover, the SMO should develop the capacity for discriminating between sensor faults and input disturbances. A pseudo-sliding form can be designed to suppress the impact of disturbances [5] and the residual error of the system can also be developed [6], [7]. Then, a SMO which introduces a fault estimation algorithm with adaptive law is proposed in this work. It is designed by the residual error and the residual error is only sensitive to sensor faults which means that the SMO is robust to unknown input disturbances. Except for the SMO, an active fault-tolerant control method is proposed. Different from the passive fault-tolerant control

The associate editor coordinating the review of this manuscript and approving it for publication was Ning Sun.

algorithm, state feedback and pseudo-inverse methods are introduced to realize active fault-tolerant compensation [8]. On the basis of adaptive sliding mode control (ASM) and fault-tolerant control distribution, an adaptive sliding mode fault-tolerant coordination (ASM-FTC) control method is proposed [9], which solves the problem of multimotor coordinate operation against the actuator faults in the 4WID system. Some advanced control strategies have also been proposed to achieve better control effects, such as RBF neural network-based supervisor control [10], deep learning based semi-supervised control [11], nonlinear control of underactuated systems [12], output feedback regulation control [13].

Different from the traditional control strategies proposed on AGV, this paper takes the AGF as the object and solves the problem of multi-sensor fault diagnosis and fault-tolerant control of AGF. Compared with conventional cars, it has more complicated model uncertainties because of the movement of the center of gravity and the variation of the cargo weight. In order to solve the multi-sensor fault and fault-tolerant control problems of AGF, firstly, considering the sensor fault and unknown disturbance, the three-degree-of-freedom forklift model is established and an equivalent fault model of the AGF system is also proposed. Secondly, an adaptive sliding mode observer is designed. The observer sets different fault thresholds for different types of sensors, so that the observer has different sensitivity characteristics to different sensor faults. In order to improve the accuracy of fault judgment, a mathematical model of sensor fault characteristics is further established, and different fault-tolerant output compensation algorithms are designed for different fault types. Finally, an active fault-tolerant control method, which is based on state feedback, is proposed. It can restore the control system to normal and maintain the stability of the control system. The main contributions of this paper are summarized as follows:

1) Based on the three-degree-of-freedom dynamic model, this paper proposes an AGF equivalent fault model, which converts the redundant parameters in the output term into the input term. Then the output is not disturbed, which facilitates the design of the observer.
2) A SMO is proposed which can detect multi-sensor faults in AGF, and the SMO is robust to unknown input interference.
3) An active fault-tolerant control method based on state feedback is proposed, which can restore the control system to normal and maintain the stability of the control system. Experiments have also proved the effectiveness of this method.

The rest of the paper is organized as follows. Section 2 gives the equivalent AGF fault model based on the three-degree-of-freedom forklift model. In Section 3, an adaptive SMO is designed. It can judge the faulty sensors according to different characteristics of faults residual. Then, a mathematical model of sensor fault characteristics is also established to further determine the type of sensor faults. In Section 4, for different fault types, an active fault-tolerant control method based on state feedback is given. And it proves that the system is stable in the sense of Lyapunov. Experimental results are discussed in Section 5 and the conclusion is presented in Section 6.

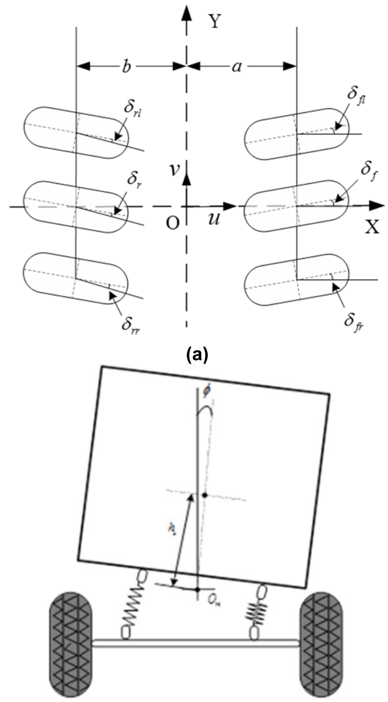

FIGURE 1. Dynamic model of forklift: (a) Top view; (b) Rear view.

II. AGF FAULT MODEL

A. THREE-DEGREE-OF-FREEDOM FORKLIFT DYNAMICS MODEL

Considering the working principle of AGF and the influence of the environment, the two-degree-of-freedom dynamics model cannot reflect the stability when the forklift is loaded. Then a three-degree-of-freedom forklift dynamics model is introduced in this manuscript [14], [15]. It can reflect its operating conditions and the stability characteristics of the AGF accurately. The horizontal ground is set as the coordinate plane. The transverse pendulum motion moves around the Z-axis, side-to-side motion move around the X-axis, and lateral motion moves along the Y-axis. The three-degree-of-freedom dynamics model of the forklift is shown in Figure 1.

The dynamics model of the forklift can be derived as [16]:

Lateral movement around the X-axis:

$$I_x\dot{p} - I_{xz}\dot{\omega} = \sum M_{xi} = L_x \tag{1}$$

Lateral motion along the y-axis:

$$m(\dot{v} + u\omega) - m_s h_s \dot{p} = \sum F_{Yi} = F_Y \tag{2}$$

Transverse pendulum motion around the Z-axis:

$$I_z\dot{\omega} - I_{xz}\dot{p} = \sum M_{zi} = M_z \tag{3}$$

where I_x is the moment of inertia around the X-axis, I_z is the moment of inertia around the Z-axis, I_{xz} is the product of inertia around the X and Z axes, h_s is the distance from the center of mass of suspension to the axis of lateral tilt, m_s is suspension mass, p is the lateral angular velocity, O_m is the center of the forklift's tilt, F_Y is the total external force in the y-axis direction, $\dot{p}$ is the lateral angular acceleration, m is the total mass of the forklift, L_x is the external moment in the X-axis direction, M_z is the total external moment on the Z-axis.

$$L_x = -c_\phi p - k_\phi \phi + m_s g h_s \sin\phi + m_s h_s u(\dot{\beta} + \omega)\cos\phi \tag{4}$$

$$F_Y = F_{Y1} + F_{Y2} + F_{Y3} + F_{Y4} \tag{5}$$

$$M_z = a(F_{Y1} + F_{Y2}) - b(F_{Y3} + F_{Y4}) \tag{6}$$

Since ϕ is small, it can be approximated as $\sin\phi = \phi$, $\cos\phi = 1$. Then the model can be derived as:

$$\begin{cases} I_x\dot{p} - I_{xz}\dot{\omega} - m_s h_s u(\dot{\beta} + \omega) = -c_\phi p - (k_\phi - m_s g h_s)\phi \\ I_z\dot{\omega} - I_{xz}\dot{p} = ak_f(\beta + \dfrac{a}{u}\omega - \delta_f - R_f\phi) \\ \qquad - bk_r(\beta - \dfrac{b}{u}\omega - \delta_r - R_r\phi) \\ mu(\dot{\beta} + \omega) - m_s h_s \dot{p} = k_f(\beta + \dfrac{a}{u}\omega - \delta_f - R_f\phi) \\ \qquad + k_r(\beta - \dfrac{b}{u}\omega - \delta_r - R_r\phi) \end{cases} \tag{7}$$

where R_f is the front axle roll steering coefficient, a, b are the distances from the mass center of the forklift to the front and rear axle respectively, c_ϕ is suspension camber damping, k_ϕ is the suspension camber angle stiffness, k_f is the equivalent lateral stiffness of the front axle tire, R_r is the rear axle roll steering coefficient, k_r is the equivalent lateral stiffness of the rear axle tire.

In the model, yaw rate ω, lateral tilt angle ϕ, lateral tilt angular velocity p, and mass center lateral deviation angle β are used as state variables, and the equivalent monorail model front wheel rotation angle δ_f is the input, namely $u(t) = \delta_f$.Thus, the equation can be written in the following form:

$$\begin{cases} \dot{x}_p(t) = A_p x_p(t) + B_p u_p(t) \\ y_p(t) = C_p x_p(t) \end{cases} \tag{8}$$

where

$$A_p = M_1^{-1}M_2, \quad B_p = M_1^{-1}M_3, \; M_3 = \begin{bmatrix} k_f & k_f a & 0 & 0 \end{bmatrix}^T,$$

$$C_p = \begin{bmatrix} 1 & 0 & 0 & 0 \\ 0 & 1 & 0 & 0 \\ 0 & 0 & 1 & 0 \\ 0 & 0 & 0 & 1 \end{bmatrix},$$

$$M_1 = \begin{bmatrix} 0 & mu & 0 & -m_s h_s \\ I_z & 0 & 0 & -I_{xz} \\ -I_{xz} & -m_s h_s u & 0 & I_x \\ 0 & 0 & 1 & 0 \end{bmatrix},$$

$$M_2 = \begin{bmatrix} \dfrac{-k_f a + k_r b}{u} - mu & -k_f - k_r & (k_f R_f + k_r R_r) & 0 \\ -\dfrac{k_f a^2 + k_r b^2}{u} & -ak_f + bk_r & (k_f a R_f - k_r b R_r) & 0 \\ m_s h_s u & 0 & -(K_\phi - m_s g h_s) & -C_\phi \\ 0 & 0 & 0 & 1 \end{bmatrix}.$$

B. EQUIVALENT FAULT MODEL

Considering the effects of the fault term and the input disturbance term, an equivalent fault model of the AGF system including sensor faults and input disturbances is developed with the three-degree-of-freedom model of the forklift.

$$\begin{cases} \dot{x}_p(\mathrm{t}) = A_p x_p(\mathrm{t}) + B_p u(t) + D_p d(t) \\ y_p(\mathrm{t}) = C_p x_p(\mathrm{t}) + E_{sp} f_s \end{cases} \tag{9}$$

where $x_p(\mathrm{t}) \in R^n$ is a state vector, D_p is a known external interference matrix, $u(\mathrm{t}) \in R^l$ is the input vector, $d(t)$ is an unknown input disturbance, f_s is a sensor fault vector, $\mathrm{y}_p(\mathrm{t}) \in R^m$ is the output vector, E_{sp} is a sensor fault distribution matrix, A_p, B_p, C_p are matrices of known constants.

To filter the output $y(\mathrm{t})$, we define a low-pass filter Z to convert sensor faults from the output to the input equivalently so that the output will not be disturbed [17]. The low-pass filter Z is:

$$\dot{z} = -A_f z + A_f y \tag{10}$$

where A_f is a stability matrix.

On the basis of (9) and (10), we get:

$$\begin{cases} \begin{bmatrix} \dot{x}_p \\ \dot{z} \end{bmatrix} = \begin{bmatrix} A_p & 0 \\ A_f C_p & -A_f \end{bmatrix} \begin{bmatrix} x_p \\ z \end{bmatrix} + \begin{bmatrix} B_p \\ A_f G_i \end{bmatrix} u \\ \qquad + \begin{bmatrix} 0 \\ A_f D_P \end{bmatrix} d(t) + \begin{bmatrix} 0 \\ A_f E_{sp} \end{bmatrix} f_{sp} \\ z = \begin{bmatrix} 0 & I_1 \end{bmatrix} \begin{bmatrix} x_p \\ z \end{bmatrix} \end{cases} \tag{11}$$

The new state variables and matrices are defined as:

$$x = \begin{bmatrix} x & z \end{bmatrix}^T, \quad y = z_i, \; A = \begin{bmatrix} A & 0 \\ A_{si}C_i & -A_{si} \end{bmatrix},$$

$$B = \begin{bmatrix} B \\ A_f G_i \end{bmatrix},$$

$$C = \begin{bmatrix} 0 & I \end{bmatrix}, \quad D = \begin{bmatrix} 0 \\ A_f d_p \end{bmatrix}, \; E_s = \begin{bmatrix} 0 \\ A_f E_{sp} \end{bmatrix}.$$

By substituting them into equation (11), we obtain the following model:

$$\begin{cases} \dot{x}(\mathrm{t}) = Ax(\mathrm{t}) + Bu(\mathrm{t}) + Dd(\mathrm{t}) + E_s f_s \\ y(\mathrm{t}) = Cx(\mathrm{t}) \end{cases} \tag{12}$$

where $x(\mathrm{t}) \in R^n$ is a state vector, D is the equivalent known external interference matrix, $\mathrm{y}(\mathrm{t}) \in R^m$ is the equivalent output vector, E_s is the equivalent sensor fault distribution matrix, A, B, and C are matrices of known constants.

In the model, all sensor faults and unknown terms can be transformed into input terms, namely, the excess parameters in the output terms can be equivalently transformed into input terms so that the output is not disturbed [18].

To design the observer, we make the following assumptions:

Hypothesis 1: $d(t)$ is bounded. It means there exists $\lambda > 0, \|d(t)\| \le \lambda$.

Hypothesis 2: There exists a matrix F such that $PD = C^T F^T$.

Hypothesis 3: There exists a matrix L such that $A_0 = A - LC$ is a stable matrix and there are two positive deterministic real symmetric matrices P, Q satisfying Lyapunov equation $A_0^T P + PA_0 = -Q$.

Hypothesis 4: There exists a positive symmetric matrix P_0 such that $E_0 = -P_0^{-1} E^T P C^{-1}$.

III. SMO DESIGN AND SENSOR FAULT DIAGNOSIS

A. SMO DESIGN

According to the AGF equivalent fault model, the following sliding mode observer can be designed to estimate the state quantity:

$$\begin{cases} \dot{\hat{x}}(t) = A\hat{x}(t) + Bu(t) + Dv + L(y - C\hat{x}) + E_s\hat{f}_s(t) \\ \hat{y}(t) = C\hat{x}(t) \end{cases} \tag{13}$$

$e_y = \hat{y}(t) - y(t)$ is defined as the observer generated residual that can be reached and maintained on the surface of the sliding mode. v is a discrete switch item defined as:

$$v = \begin{cases} -\beta_h \dfrac{Fe_y}{\|Fe_y\|}, & e_y \neq 0 \\ 0, & e_y = 0 \end{cases} \tag{14}$$

Since the residual only contains fault information, a fault estimation algorithm is designed which can be adaptively adjusted for better tracking performance [19]. It can be derived as:

$$\dot{\hat{f}}_s = E_0 e_y \tag{15}$$

where E_0 is a suitable matrix satisfying hypothesis 4. Fault estimation is defined as $\tilde{f}_s(t) = \hat{f}_s(t) - f_s(t)$, the state observation error is defined as $e(t) = \hat{x}(t) - x(t)$. In summary, the system estimates the error equation as follows:

$$\begin{cases} \dot{e}(t) = (A - LC)e(t) + D(v - d(t)) + E_s\tilde{f}_s \\ e_y = Ce(t) \end{cases} \tag{16}$$

From Hypothesis 3, the equation can be written as:

$$\begin{cases} \dot{e}(t) = A_0 e(t) + D(v - d(t)) + E_s\tilde{f}_s(t) \\ e_y = Ce(t) \end{cases} \tag{17}$$

Theorem 1: Considering the fault model (17), the sensor fault estimate error $\tilde{f}_s$ and the state observation error e are both stabilized at 0 under the condition that Hypotheses 1 to 4 are both met.

Proof: When $f_s \neq 0$, the Lyapunov function is selected:

$$V = e^T Pe + \tilde{f}_s^T P\tilde{f}_s \tag{18}$$

and its derivative is calculated as:

$$\begin{aligned} \dot{V} &= \dot{e}^T Pe + e^T P\dot{e} + \dot{\tilde{f}}_s^T P\tilde{f}_s + \tilde{f}_s^T P\dot{\tilde{f}}_s \\ &= e^T (A_0^T P + PA_0)e + 2e^T PD(v - d) + 2e^T PE\tilde{f}_s \\ &\quad + 2\tilde{f}_s^T PE\dot{\tilde{f}}_s \\ &= -e^T Qe + 2(FCe)^T (v - d) + 2\tilde{f}_s^T (E^T Pe + P\dot{\tilde{f}}_s) \\ &\le -e^T Qe - 2(Fe_y)^T \beta_h \frac{Fe_y}{\|Fe_y\|} + 2\|Fe_y\| \|d\| \\ &\quad + 2\tilde{f}_s^T (E^T Pe + P_0\dot{\tilde{f}}_a) \\ &\le -2\|Fe_y\| (\beta_h - \|d\|) + 2\tilde{f}_s^T (E^T Pe + P_0\dot{\tilde{f}}_s) \\ &\le 2\tilde{f}_s^T (E^T Pe + P_0\dot{\tilde{f}}_s) \end{aligned}$$

Thus when $\dot{\tilde{f}}_s = -P_0^{-1} E^T Pe = E_0 e_y$, it is guaranteed that $\dot{V} \le 0$. Therefore, both the fault estimation error $\tilde{f}_s$ and the state observation error e converge in the zero domain.

From the proof of Theorem 1 and Eq. (17), the residual $e_y(t) = \hat{y}(t) - y(t)$ is not affected by the unknown input perturbation and it will only be affected by the fault f_s. Therefore, the residuals are only sensitive to faults occurring in system components, thus it proves that the robustness of the method to unknown input perturbations. When the sensor does not fail, the state observation error converges to zero, so it can be used as a fault detection observer. At the same time, by setting specific thresholds for different types of sensors based on the size of their respective eigenvectors at the time of the fault, it is possible to accurately determine the fault in different situations. The following thresholds can be set to determine if the system is malfunctioning:

$$k(t) = \begin{cases} \|e_{y0}\|_2 \le \mu_i & \text{No fault occurs} \\ \|e_{y0}\|_2 > \mu_i & \text{Fault occurs} \end{cases} \tag{19}$$

where μ_i is the maximum value of the residuals that would have occurred if each sensor had not failed.

Note 1: Inserting the discontinuous switching term into the observer can effectively suppress the unknown input perturbation, thus making the observer robust to the unknown input perturbation. However, inserting the discontinuous switching term causes the sliding mode control to be discontinuous and the system will generate high-frequency jitter and disturbance. This problem can be solved by replacing the discontinuous switching term with a saturation function to suppress the jitter. As follows:

$$v = -\beta_h \frac{Fe_y}{\|Fe_y\| + \delta} \tag{20}$$

where δ is a small constant.

B. SENSOR FAULT DIAGNOSIS AND FAULT CHARACTERIZATION MODELING

The accuracy of sensor measurement data is critical to the safety of the entire AGF system, so the main sensor faults involved in AGF systems are classified. The observer method described above can determine which sensor has failed and

TABLE 1. ***i*** **represents the sensor.**

Symbol	Represented Sensors
$i = 1$	the left front wheel angle sensor
$i = 2$	the right front wheel angle sensor
$i = 3$	the left rear wheel angle sensor
$i = 4$	the right rear wheel angle sensor
$i = 5$	the yaw rate sensor
$i = 6$	the tilt angle velocity sensor

therefore the type of sensor faults that has occurred, allowing for fault-tolerant compensation and active fault-tolerant control of the sensor.

Definition: type of sensor faults

Sensor Noise Faults: During the measurement and transmission process, the signal is disturbed by the external environment, and the output value contains a lot of noise compared to the normal value.

Sensor Stuck Faults: When the sensor is damaged, powered down, or suddenly short-circuited, its output value is stuck at a fixed value.

Sensor Drift Faults: When the sensor is working, there is a problem with the connection of its internal components, and there is a constant deviation between the output value and the normal value.

To accurately determine the type of sensor faults, it is necessary to analyze the sensor fault characteristics and then model each type of sensor fault. The normal sensor measurement model is as follows:

$$y_{mij} = y_{rij} + \Delta y_{ij} \tag{21}$$

where y_{mi} is the measured value of the sensor, y_{ri} is the real value, Δy_i is the measurement error of the sensor, i are different types of sensors, j is the type of sensor fault.

Each sensor has its threshold value under different fault conditions, and when the corresponding threshold value is exceeded, it is determined what kind of fault occurs in that sensor.

The above introduces residuals as a fault determination, but only considering the variation of residuals to determine the type of fault is not sufficient to make a specific distinction between sensor faults. By analyzing the characteristics of the sensor measurement data and establishing a mathematical model of the sensor fault characteristics, the fault determination accuracy can be improved.

Residual definition:

$$R_{fsi} = \begin{cases} \delta_{fm} - \delta_{fes} & i = 1, 2, 3, 4 \\ \omega_{fm} - \omega_{fes} & i = 5 \\ p_{fm} - p_{fes} & i = 6 \end{cases} \tag{22}$$

where R_{fsi} is the residual, δ_{fm} is the measured value, δ_{fes} is the observer estimate, i is the sensor type, As shown in Table 1:

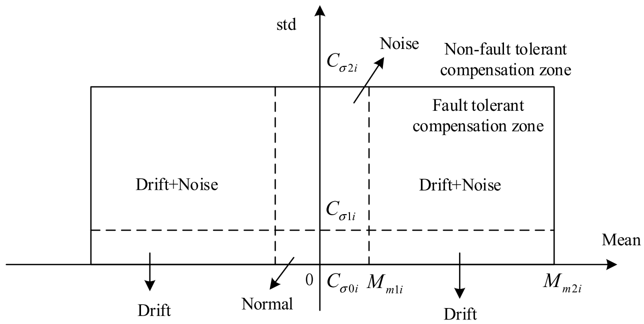

FIGURE 2. **Sensor faults zone.**

1) SENSOR NOISE FAULT MODEL

$$\begin{cases} y_{mij} = y_{rj} + \Delta y_{ij} \\ \text{Std}\left(R_{fsi}\right) \in [C_{\sigma 1i}, C_{\sigma 2i}] \\ \left|\text{Mean}\left(R_{fsi}\right)\right| \in [0, M_{m1i}] \end{cases} \tag{23}$$

where y_{rj} is the real value, $C_{\sigma 2i}$, M_{mli} are the upper limits of the standard deviation of the residuals that can be tolerated by each sensor, Δy_{ij} is a noise disturbance in the sensor, $C_{\sigma 1i}$ is the lower limit of the residual standard deviation of the tolerable range of noise fault compensation for each sensor.

2) SENSOR STUCK FAULT MODEL

$$\begin{cases} y_{mij} = C_i \\ \text{Mean}\left(R_{fsi}\right) = M_{si} \\ \text{Std}\left(R_{fsi}\right) \leq S_{\sigma 0i} \end{cases} \tag{24}$$

where C_i is a fixed constant value, $S_{\sigma 0i}$ is the upper limit of the measured value.

3) SENSOR DRIFT FAULT MODEL

$$\begin{cases} y_{mij} = y_{rij} + \Delta R_{ij} \\ \text{Std}\left(R_{fsi}\right) \in [C_{\sigma 0i}, C_{\sigma 1i}] \\ \left|\text{Mean}\left(R_{fsi}\right)\right| \in [M_{m1i}, M_{m2i}] \end{cases} \tag{25}$$

where ΔR_{ij} is the error under drift interference, M_{m2i} is the upper limit of the sensor's tolerance for compensating residual standard deviation, $C_{\sigma 0i}$ is the lower limit of the residual standard deviation of the fault-tolerant compensation range for each sensor drift.

In this paper, we mainly study the noise fault, jam fault, and drift fault, and after determining the specific fault type of each sensor, the fault-tolerant compensation algorithm deals with them. The measurement data is partially valid when the sensor has noise and drift faults, while the measurement data is invalid when the sensor has stuck faults and needs to be dealt with first. In practice, according to the fault characteristic model of each sensor, the fault can be divided into three areas: the fault tolerant compensation area, the normal working area, and the non-fault tolerant compensation area. As shown in Figure 2:

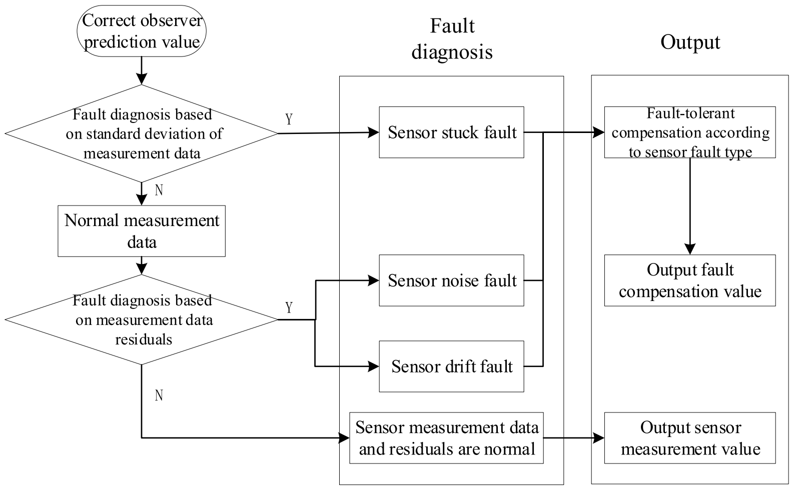

FIGURE 3. **Fault-tolerant compensation flow chart.**

IV. ACTIVE FAULT TOLERANT CONTROL ALGORITHM DESIGN

A. FAULT DIAGNOSIS OUTPUT PROCESSING FLOW

According to the different types of sensor faults, the fault-tolerant compensation method is designed as shown in Figure 3:

1) ACTIVE FAULT-TOLERANT CONTROL ALGORITHM BASED ON STATE FEEDBACK

The fault-tolerant compensation control algorithm can make the output close to the output value of a normal system. But the fault-tolerant compensation method does not consider the effects of system parameter uncertainty. Introducing state feedback and pseudo-reverse method, an active fault-tolerant control method for the AGF uncertainty system is proposed, which can effectively ensure the stability of the AGF control system by restoring the sensor output value to a near-normal operating state in the event of a fault.

Based on the fault system model (12) and the fault estimation deviation relationship $\tilde{f}_s(t) = \hat{f}_s(t) - f_s(t)$, the active fault-tolerant control ratio is designed as follow:

$$U(t) = Kx(t) + BE_s\tilde{f}_s \tag{26}$$

To ensure the built active fault-tolerant controller stable, some Hypotheses are proposed as follow:

Hypothesis 1: $d(t)$ is bounded. It means there exists $\lambda > 0$, $\|d(t)\| \le \lambda$.

Hypothesis 2: There exists a minimal value τ such that $\beta < \lambda + \tau$.

Hypothesis 3: There exists a matrix F such that $PD = C^T F^T$.

Hypothesis 4: There exists a matrix L such that $A_0 = A - LC$ is a stable matrix and there are two positive deterministic real symmetric matrices P, Q satisfying Lyapunov's equation $A_0^T P + PA_0 = -Q$.

Hypothesis 5: There exists a positive symmetric matrix P_0 such that $E_0 = -P_0^{-1}E^T PC^{-1}$.

Hypothesis 6: There exists fault estimation deviation $e(t)$ such that $f_s(t) = \frac{1}{c}e^{ce(t)}e(t) - \frac{1}{c^2}e^{ce(t)}e(t) + c_1$.

Hypothesis 7: There exists external disturbance $d(t)$ such that $\|Fe_y\| \le \frac{\alpha\|D\|^2\|d(t)\|^2}{2(\vartheta - \|d(t)\|)}$. where $c = 0.5\|E_s\|^2$, c_1, α, and β are arbitrary constants.

As defined above: the fault estimation error is defined as $\tilde{f}_s(t) = \hat{f}_s(t) - f_s(t)$, the state observation error is defined as $e(t) = \hat{x}(t) - x(t)$,the output estimation error is defined as $e_y(t) = \hat{y}(t) - y(t)$.Introduce the feedback control rate into the fault equation, where the closed-loop expression of the fault equation is as follows:

$$\begin{cases} \dot{x}(t) = Ax(t) + Bkx(t) - BB^t E_s\hat{f}_s + Dd(t) + E_s f_s \\ y(t) = Cx(t) \end{cases} \tag{27}$$

Simplified:

$$\begin{cases} \dot{x}(t) = (A + Bk)x(t) - E_s(\hat{f}_s - f_s) + Dd(t) \\ y(t) = Cx(t) \end{cases} \tag{28}$$

The discontinuous switching term v is defined as:

$$v = \begin{cases} -\vartheta \dfrac{Fe_y}{\|Fe_y\|}, & e_y \ne 0 \\ 0, & e_y = 0 \end{cases} \tag{29}$$

Theorem 2: Considering the fault model (28), the sensor fault estimate error $\tilde{f}_s$ and the state observation error e are both stabilized at 0 under the condition that hypotheses 1 to 7 are both met.

Proof: The Lyapunov function is selected:

$$V = e^T Te + \tilde{f}_s^T P\tilde{f}_s + x^T Px \tag{30}$$

and its derivative is calculated as:

$$\begin{aligned} \dot{V} &= \dot{e}^T Pe + e^T P\dot{e} + \dot{\tilde{f}}_s^T P\tilde{f}_s + \tilde{f}_s^T P\dot{\tilde{f}}_s + 2x^T P\dot{x} \\ &= e^T Qe + 2(FCe)^T(v - d) + 2\tilde{f}_s^T(E^T Pe + p\dot{\tilde{f}}_s) + 2x^T P\dot{x} \\ &= e^T Qe + 2(FCe)^T(v - d) + 2\tilde{f}_s^T(E^T Pe + p\dot{\tilde{f}}_s) \end{aligned}$$

$$
\begin{aligned}
&+2x^T P\left(Ax(t)+Bkx(t)-BB^t E_s\hat{f}_s+Dd(t)+E_s f_s\right)\\
&= e^T Qe+2(FCe)^T(v-d)+2\tilde{f}_s^T(E^T Pe+p\dot{\tilde{f}}_s)\\
&\quad +2x^T P(A+BK)x+2xPDd(t)-2x^T PE_s\hat{f}_s\\
&\leq e^T Qe+2(FCe)^T(v-d)+2\tilde{f}_s^T(E^T Pe+p\dot{\tilde{f}}_s)\\
&\quad -\lambda\min(Q_1)||x||^2\\
&\quad +\frac{1}{\alpha}\|P\|^2\|x\|^2+\alpha\|D\|^2\|d(t)\|^2+\frac{1}{\chi}\|P\|^2\|x\|^2\\
&\quad +\chi\|E_s\|^2\left\|\tilde{f}_s\right\|^2\\
&\leq e^T Qe+2(FCe)^T(v-d)+2\tilde{f}_s^T(E^T Pe+p\dot{\tilde{f}}_s)\\
&\quad +\chi\|E_s\|^2\left\|\tilde{f}_s\right\|^2-(\lambda\min(Q_1)-\frac{1}{\alpha}\|P\|^2-\frac{1}{\chi}\|P\|^2)||x||^2\\
&\quad +\alpha\|D\|^2\|d(t)\|^2\\
&\leq e^T Qe+2(FCe)^T(v-d)+2\tilde{f}_s^T(E^T Pe+p\dot{\tilde{f}}_s)\\
&\quad -2||Fe_y||\,(\vartheta-\|d(t)\|)\\
&\quad +\alpha\|D\|^2\|d(t)\|^2+\alpha\|D\|^2\|d(t)\|^2+\chi\|E_s\|^2\left\|\tilde{f}_s\right\|^2\\
&= e^T Qe+2(FCe)^T(v-d)+2\tilde{f}_s^T(E^T Pe+p\dot{\tilde{f}}_s)\\
&\quad +\alpha\|D\|^2\|d(t)\|^2\\
&\quad -2||Fe_y||\left(\vartheta-\|d(t)\|-\frac{1}{2||Fe_y||}\alpha\|D\|^2\|d(t)\|^2\right)\\
&\quad +\chi\|E_s\|^2\left\|\tilde{f}_s\right\|^2\\
&\leq e^T Qe+2(FCe)^T(v-d)+2\tilde{f}_s^T(E^T Pe+p\dot{\tilde{f}}_s)\\
&\quad +\alpha\|D\|^2\|d(t)\|^2+\chi\|E_s\|^2\left\|\tilde{f}_s\right\|^2\\
&= e^T Qe+2(FCe)^T(v-d)+2\tilde{f}_s^T(E^T Pe+p\dot{\tilde{f}}_s)\\
&\quad +\alpha\|D\|^2\|d(t)\|^2+\chi\|E_s\|^2\tilde{f}_s^T\tilde{f}_s\\
&\leq -e^T Qe+2(Fe_y)^T(v-d)+2\tilde{f}_s^T\\
&\quad \times\left(E^T Pe+p\dot{\tilde{f}}_s+\chi\|E_s\|^2\tilde{f}_s\right)+\alpha\|D\|^2\|d(t)\|^2\\
&\leq -e^T Qe+2(Fe_y)^T(v-d)+\alpha\|D\|^2\|d(t)\|^2\\
&\leq -2||Fe_y||\left(\beta_h-\frac{Fe_y}{||Fe_y||}\right)+2\|Fe_y\|\,\|d(t)\|\\
&\quad +\alpha\|D\|^2\|d(t)\|^2
\end{aligned}
$$

Thus $\dot{V}<0$. Therefore, both the fault estimation error $\tilde{f}_s$ and the state observation error e converge in the zero domain. It proves that the system is stable [18], [20].

V. EXPERIMENT RESULTS

The MIMA laser-guided AGF is used as the experimental platform, which is equipped with manual driving and automatic navigation modes and four-wheel steering. The experimental platform is shown in Figure 4. Based on the given sensor fault type diagnosis strategy, the corresponding fault-tolerant strategy, and the AGF fault model, the following sensor experiments are designed to verify the effectiveness of the fault-tolerant compensation algorithm.

FIGURE 4. AGF experimental platform.

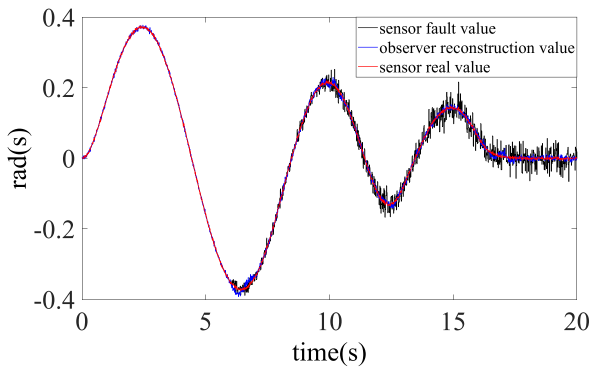

FIGURE 5. Output (including noise).

A. SENSOR FAULT DIAGNOSIS EXPERIMENTS

The left front wheel angle sensor is used as a diagnostic object. The sensor real value, the sensor fault value, and the observer reconstruction value are observed when the sensor has a noise fault, a stuck fault, and a drift fault, respectively. where $C_{m11}=5\times10^{-3}rad$, $C_{\sigma11}=5\times10^{-3}rad$, $C_{\sigma01}=2\times10^{-7}rad$.

1) When a noise fault occurs in the sensor at the 6th second, it can be seen in Figure 5 that the output value noise gradually increases with time and the observer can achieve noise reduction processing to restore the sensor real value.

2) When the sensor stuck fault and drift fault occur at the 8th second respectively, the sensor measured value generates an error, and the sensor output value reconfiguration is performed by the above-mentioned observer. It can be seen from Figure 6 and Figure 7 that the observer can achieve the sensor value reconstruction and satisfy the fault-tolerant control requirements.

B. ACTIVE FAULT-TOLERANT CONTROL EXPERIMENTS

In this experiment, we consider that the roll rate sensor, the left front wheel angle sensor, and the yaw rate sensor fail, respectively. In the experiment, we input the value of 0.6 rad/s for the front wheel steering angle, where

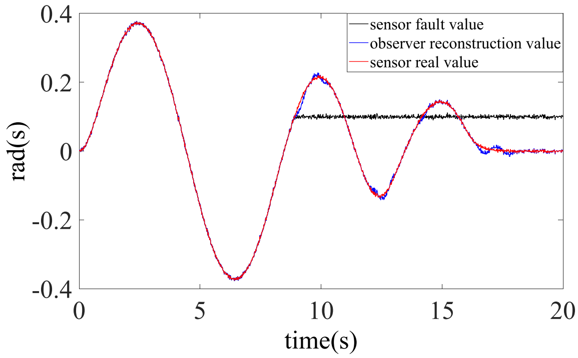

FIGURE 6. Stuck fault compensation.

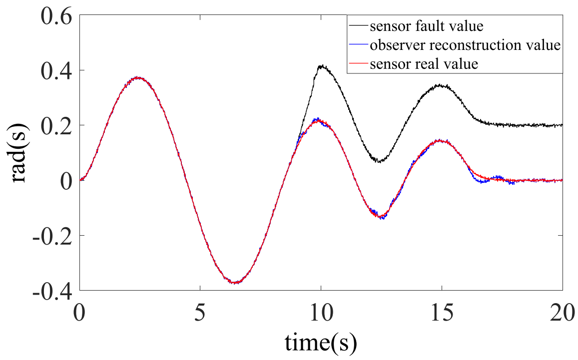

FIGURE 7. Drift fault compensation.

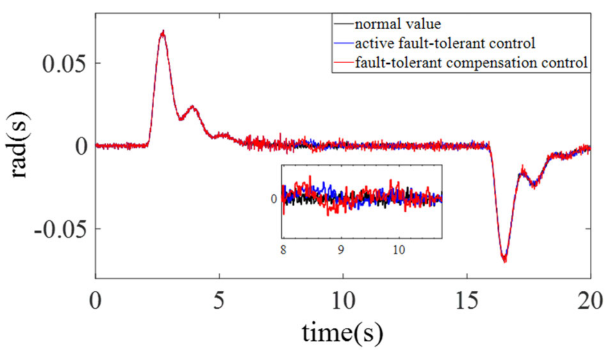

FIGURE 8. Tracking curve of roll angle under different fault tolerance modes.

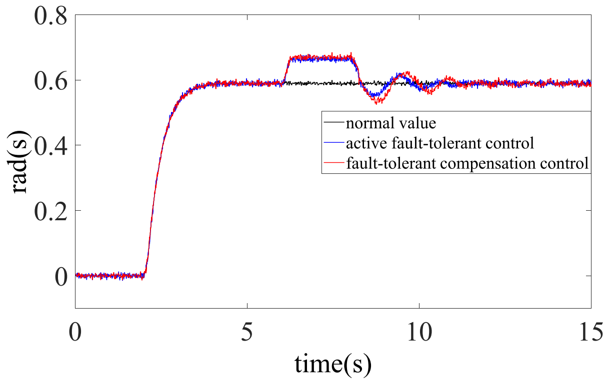

FIGURE 9. Tracking curve of left front wheel angle under different fault tolerance modes.

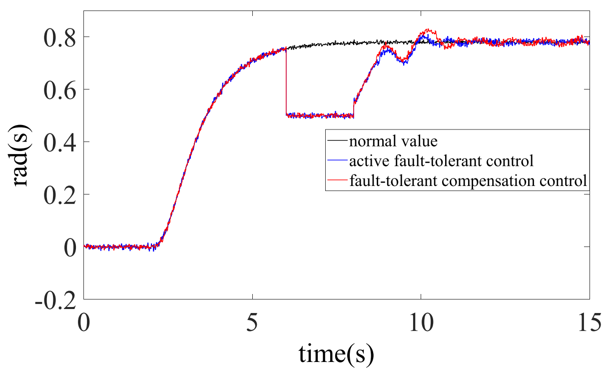

FIGURE 10. Tracking curve of yaw rate under different fault tolerant modes.

The noise Fault occurs in the roll rate sensor at the 6th second;

The drift fault occurs in the left front wheel angle sensor at the 6th second;

The stuck fault occurs in the yaw rate sensor at the 6th second: stuck at 0.5 rad/s.

As shown in Figure 8, at the 6th second, a noise fault occurs in the roll rate sensor, and a large amount of white noise floods the original output in the fault-tolerant compensation control and active fault-tolerant control curves. In the 8th second, fault-tolerant compensation control and active fault-tolerant control based on state feedback are added. They can suppress the noise to a certain extent, and the active fault-tolerant control is more effective than the fault-tolerant control.

As shown in Figure 9, at the 6th second, the drift fault occurs in the left front wheel angle sensor, then the fault-tolerant compensation curve and active fault-tolerant control curve fluctuate significantly and deviate from the normal value. At the 8th second, we introduce the fault-tolerant compensation and active fault-tolerant control. Both of them are effective and the left front wheel rotation angle value is extremely close to the normal value after about 2 seconds. It proves that they could return the system to normal operation. However, the fluctuation of the curve of the fault-tolerant compensation control is larger than that of the active fault-tolerant control. It means that the fault-tolerant compensation control is not as effective as the active fault-tolerant control.

As shown in Figure 10, at the 6th second, the stuck fault occurs in the yaw rate sensor, and the fault-tolerant compensation value and the active fault-tolerant control value change significantly and deviate from the normal value. At the 8th second, the active fault-tolerant control and the fault-tolerant compensation control are introduced.

They can also implement fault tolerant control but compared with the fault-tolerant compensation control, the active fault-tolerant control can return to the normal value more quickly with less fluctuation. It means that the fault-tolerant compensation is not as effective as the active fault-tolerant control algorithm.

VI. CONCLUSION

As an important means of transportation of cargos, the safety of AGF is the primary factor that must be considered. With the development of electronic components, fault diagnosis and fault-tolerant control technology have become extremely important to ensure safety.

Firstly, according to the forklift three-degree-of-freedom model, an equivalent fault model of the AGF system including sensor faults and input disturbances is established. It considers the influence of the fault item and the unknown input disturbance item. An output low-pass filter is also introduced to convert sensor faults and unknown disturbance items into input items so that the output is not disturbed.

For the fault detection of multiple AGF sensors, a SMO with adaptive regulation law is adopted. As sensors have different working conditions, different residual thresholds are set so that the designed observer can be sensitive to specific sensor faults. At the same time, the characteristics of the residual signal are used to design the adaptive rate and the continuous switch is introduced to effectively suppress the unknown input disturbance. It means that the observer is robust to unknown input disturbances. In order to suppress the sliding mode jitter, the discontinuous switching item is also replaced with a saturation function. Then, the main sensor characteristics of AGF are analyzed, and equivalent sensor noise fault, drift fault, and stuck fault characteristic models are established. After judging which sensor has a fault, we can further use the fault characteristic model to analyze which type of fault the sensor has.

Then, an active fault-tolerant control method for the AGF uncertain system is proposed. It introduces the method of state feedback and pseudo-inverse and the active fault-tolerant control rate is designed according to the fault system model and the error relationship of the fault estimation. It can restore the sensor output value to normal when a fault occurs and ensure system stability.

Finally, experiments verify the effectiveness of the proposed method.

ACKNOWLEDGMENT

The authors are grateful to senior engineers Junliang Guo, Zijian Fang, Pengfei Li, Xingzhi Fang, and Weilin Lv for their cooperation and helpful suggestions.

REFERENCES

[1] R. Wang and J. Wang, ''Fault-tolerant control with active fault diagnosis for four-wheel independently driven electric ground vehicles,'' *IEEE Trans. Veh. Technol.*, vol. 60, no. 9, pp. 4276–4287, Nov. 2011.

[2] H. Yang, V. Cocquempot, and B. Jiang, ''Optimal fault-tolerant path-tracking control for 4WS4WD electric vehicles,'' *IEEE Trans. Intell. Transp. Syst.*, vol. 11, no. 1, pp. 237–243, Mar. 2010.

[3] S. Laghrouche, J. Liu, F. S. Ahmed, M. Harmouche, and M. Wack, ''Adaptive second-order sliding mode observer-based fault reconstruction for PEM fuel cell air-feed system,'' *IEEE Trans. Control Syst. Technol.*, vol. 23, no. 3, pp. 1098–1109, May 2015.

[4] I. Boulaabi, A. Sellami, and F. B. Hmida, ''Robust delay-derivative-dependent sliding mode observer for fault reconstruction : A diesel engine system application,'' *Circuits, Syst., Signal Process.*, vol. 35, no. 7, pp. 2351–2372, Jul. 2016.

[5] L. Gou, Y. Shen, H. Zheng, and X. Zeng, ''Multi-fault diagnosis of an aero-engine control system using joint sliding mode observers,'' *IEEE Access*, vol. 8, pp. 10186–10197, 2020.

[6] K. Zhang, B. Jiang, X.-G. Yan, and J. Shen, ''Interval sliding mode observer based incipient sensor fault detection with application to a traction device in China railway high-speed,'' *IEEE Trans. Veh. Technol.*, vol. 68, no. 3, pp. 2585–2597, Mar. 2019.

[7] W. Chen and M. Saif, ''Observer-based strategies for actuator fault detection, isolation and estimation for certain class of uncertain nonlinear systems,'' *IET Control Theory Appl.*, vol. 1, no. 6, pp. 1672–1680, Nov. 2007.

[8] S. S. Tohidi, A. K. Sedigh, and D. Buzorgnia, ''Fault tolerant control design using adaptive control allocation based on the pseudo inverse along the null space,'' *Int. J. Robust Nonlinear Control*, vol. 26, no. 16, pp. 3541–3557, Nov. 2016.

[9] D. Zhang, G. Liu, H. Zhou, and W. Zhao, ''Adaptive sliding mode fault-tolerant coordination control for four-wheel independently driven electric vehicles,'' *IEEE Trans. Ind. Electron.*, vol. 65, no. 11, pp. 9090–9100, Nov. 2018.

[10] Y. Sun, J. Xu, G. Lin, W. Ji, and L. Wang, ''RBF neural network-based supervisor control for maglev vehicles on an elastic track with network time-delay,'' *IEEE Trans. Ind. Informat.*, early access, Oct. 19, 2020, doi: 10.1109/TII.2020.3032235.

[11] Y. Sun, J. Xu, H. Wu, G. Lin, and S. Mumtaz, ''Deep learning based semi-supervised control for vertical security of maglev vehicle with guaranteed bounded airgap,'' *IEEE Trans. Intell. Transp. Syst.*, early access, Jan. 1, 2021, doi: 10.1109/TITS.2020.3045319.

[12] H. Chen and N. Sun, ''Nonlinear control of underactuated systems subject to both actuated and unactuated state constraints with experimental verification,'' *IEEE Trans. Ind. Electron.*, vol. 67, no. 9, pp. 7702–7714, Sep. 2020.

[13] H. Chen and N. Sun, ''An output feedback approach for regulation of 5-DOF offshore cranes with ship yaw and roll perturbations,'' *IEEE Trans. Ind. Electron.*, early access, Feb. 2, 2021, doi: 10.1109/TIE.2021.3055159.

[14] C. Huang, F. Naghdy, and H. Du, ''Observer-based fault-tolerant controller for uncertain steer-by-wire systems using the delta operator,'' *IEEE/ASME Trans. Mechatronics*, vol. 23, no. 6, pp. 2587–2598, Dec. 2018.

[15] X. Zhang and B. Xiao, ''Research on active steering control strategy based on sideslip angle estimation for a steering-by-wire forklift,'' *IEEJ Trans. Electr. Electron. Eng.*, vol. 14, no. 6, pp. 908–916, Jun. 2019.

[16] Z. Jiang and B. Xiao, ''LQR optimal control research for four-wheel steering forklift based-on state feedback,'' *J. Mech. Sci. Technol.*, vol. 32, no. 6, pp. 2789–2801, Jun. 2018.

[17] X. Li and W. Zhang, ''An adaptive fault-tolerant multisensor navigation strategy for automated vehicles,'' *IEEE Trans. Veh. Technol.*, vol. 59, no. 6, pp. 2815–2829, Jul. 2010.

[18] J. Park, L. Wang, J. M. Dawson, L. A. Hornak, and P. Famouri, ''Sliding mode-based microstructure torque and force estimations using MEMS optical monitoring,'' *IEEE Sensors J.*, vol. 5, no. 3, pp. 546–552, Jun. 2005.

[19] H. Yang, V. Cocquempot, and B. Jiang, ''Robust fault tolerant tracking control with application to hybrid nonlinear systems,'' *IET Control Theory Appl.*, vol. 3, no. 2, pp. 211–224, Feb. 2009.

[20] H. Wang, H. Kong, Z. Man, D. M. Tuan, Z. Cao, and W. Shen, ''Sliding mode control for steer-by-wire systems with AC motors in road vehicles,'' *IEEE Trans. Ind. Electron.*, vol. 61, no. 3, pp. 1596–1611, Mar. 2014.

[21] H. Yang and S. Yin, ''Actuator and sensor fault estimation for time-delay Markov jump systems with application to wheeled mobile manipulators,'' *IEEE Trans. Ind. Informat.*, vol. 16, no. 5, pp. 3222–3232, May 2020.

[22] M. Li and Y. Chen, ''Robust adaptive sliding mode control for switched networked control systems with disturbance and faults,'' *IEEE Trans. Ind. Informat.*, vol. 15, no. 1, pp. 193–204, Jan. 2019.

[23] J. Zhao, B. Jiang, X. Fei, Z. Gao, and Y. Xu, ''Adaptive sliding mode backstepping control for near space vehicles considering engine faults,'' *J. Syst. Eng. Electron.*, vol. 29, no. 2, pp. 343–351, Apr. 2018.

[24] L. J. Chen, C. Edwards, and H. Alwi, ''Sensor redundancy based FDI using an LPV sliding mode observer,'' *IET Control Theory Appl.*, vol. 12, no. 14, pp. 1956–1963, Sep. 2018.

[25] X. B. Zhang and Z. P. Zhou, ''Integrated fault estimation and fault tolerant attitude control for rigid spacecraft with multiple actuator faults and saturation,'' *IET Control Theory Appl.*, vol. 13, no. 15, pp. 2365–2375, Oct. 2019.

HANGUO KANG received the B.S. degree from the Department of Automation, School of Computer Science, South-Central University for Nationalities, Wuhan, China, in 2018. He is currently pursuing the M.S. degree in control theory and control engineering. His current research interests include forklift fault diagnosis and isolation, fault-tolerant control, sliding mode control, and wireless sensor network localization.

BENXIAN XIAO received the Ph.D. degree from the Department of Automation, School of Electrical Engineering and Automation, Hefei University of Technology, Hefei, China, in 2004. He is currently a Professor of control theory and control engineering subjects. His current research interests include fault diagnosis, fault-tolerant control, intelligent control, automotive steering control systems, and system modeling and simulation.

YOYUAN NI received the B.Eng. and Ph.D. degrees in electrical engineering from the Hefei University of Technology, Hefei, China, in 1999 and 2006, respectively. Since 2006, he has been with Hefei University of Technology, where he is currently an Associate Professor. His current research interest includes design and control of electric machines.

WEIDONG JIANG (Member, IEEE) received the B.S. and Ph.D. degrees in electrical engineering from the Hefei University of Technology, Hefei, China, in1999 and 2004, respectively. Since June 2004, he has been with the School of Electrical Engineering and Automation, Hefei University of Technology, where he is currently a Professor. His research interests include electrical machines and their control systems, power electronics, and electric drives.

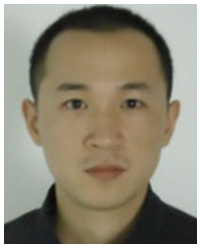

JINPING WANG (Member, IEEE) received the B.S. degree in electronic and information engineering and the Ph.D. degree in electrical engineering from Southwest Jiaotong University, Chengdu, China, in 2007 and 2013, respectively. Since June 2013, he has been with the School of Electrical Engineering and Automation, Hefei University of Technology, Hefei, China, where he is currently an Associate Professor. His main research interests include modeling, analysis, control, and applications of switching-mode power supplies.

ZHENG SUN received the B.S. degree in automation and the M.S. degree in control engineering from the School of Electrical Engineering and Automation, Hefei University of Technology, Hefei, China, in 2016 and 2020, respectively. His current research interests include forklift fault diagnosis and isolation, fault-tolerant control, sliding mode control, and intelligent control.

ZHILU ZHANG received the B.S. degree from the Department of Automation, School of Electrical Engineering and Automation, Hefei University of Technology, Hefei, China, in 2016. He is currently pursuing the M.S. degree in control theory and control engineering. His current research interests include fault diagnosis, fault-tolerant control, sliding mode control, and vehicle stability control.